Cancer Research

APOBEC3B Upregulation and Genomic Mutation Patterns in Serous Ovarian Carcinoma

Brandon Leonard[1,2], Steven N. Hart[3], Michael B. Burns[1,2], Michael A. Carpenter[1,2], Nuri A. Temiz[1,2], Anurag Rathore[1,2], Rachel I. Vogel[2], Jason B. Nikas[2], Emily K. Law[1,2], William L. Brown[1,2], Ying Li[3], Yuji Zhang[3], Matthew J. Maurer[3], Ann L. Oberg[3], Julie M. Cunningham[4], Viji Shridhar[5], Debra A. Bell[5], Craig April[13], David Bentley[13], Marina Bibikova[13], R. Keira Cheetham[13], Jian-Bing Fan[13], Russell Grocock[13], Sean Humphray[13], Zoya Kingsbury[13], John Peden[13], Jeremy Chien[11], Elizabeth M. Swisher[12], Lynn C. Hartmann[6], Kimberly R. Kalli[10], Ellen L. Goode[7], Hugues Sicotte[7], Scott H. Kaufmann[8,9], and Reuben S. Harris[1,2]

Abstract

Ovarian cancer is a clinically and molecularly heterogeneous disease. The driving forces behind this variability are unknown. Here, we report wide variation in the expression of the DNA cytosine deaminase APOBEC3B, with elevated expression in the majority of ovarian cancer cell lines (three SDs above the mean of normal ovarian surface epithelial cells) and high-grade primary ovarian cancers. APOBEC3B is active in the nucleus of several ovarian cancer cell lines and elicits a biochemical preference for deamination of cytosines in 5′-TC dinucleotides. Importantly, examination of whole-genome sequence from 16 ovarian cancers reveals that *APOBEC3B* expression correlates with total mutation load as well as elevated levels of transversion mutations. In particular, high *APOBEC3B* expression correlates with C-to-A and C-to-G transversion mutations within 5′-TC dinucleotide motifs in early-stage high-grade serous ovarian cancer genomes, suggesting that APOBEC3B-catalyzed genomic uracil lesions are further processed by downstream DNA "repair" enzymes including error-prone translesion polymerases. These data identify a potential role for APOBEC3B in serous ovarian cancer genomic instability. *Cancer Res; 73(24); 7222–31. ©2013 AACR.*

Introduction

Ovarian cancer remains the deadliest gynecologic malignancy in the United States, with an estimated 22,300 new cases and 15,500 deaths in 2012 (1). Although multiple histologic subtypes of ovarian cancer are recognized, including clear cell and endometrioid, the most common and deadly form is serous ovarian cancer. This disease usually escapes detection until it has spread throughout the peritoneal cavity. Previous analyses of high-grade, mostly late-stage serous ovarian cancers have demonstrated mutational inactivation of *TP53* in 95% of cases (2). Mutations in several other genes, including *BRCA1*, *BRCA2*, and *CDK12*, also collectively occur in approximately one quarter of high-grade serous ovarian cancers; in addition, genomic instability, as manifested by large amplifications and deletions, is common (2, 3). In contrast, clear cell and endometrioid ovarian cancers are characterized by mutations *PIK3CA* and *ARID1A*, with endometrioid ovarian cancers also having frequent *CTNNB1* mutations or *PTEN* loss.

Despite this genetic heterogeneity, ovarian cancers are typically treated with the same chemotherapy after surgical debulking. Most ovarian cancers respond initially to DNA cross-linking chemotherapeutic agents, such as carboplatin (4, 5). However, drug resistance commonly develops, with disease recurrence occurring at an average of 18 months after initiating therapy and only 44% of patients remaining alive 5 years after diagnosis (1). Mechanisms for resistance remain poorly understood, but have been attributed, at least in the case of some *BRCA1/2* mutant tumors, to the acquisition of further mutations (6). The mechanisms responsible for the mutational evolution of these cancers are not completely understood.

We recently discovered a major role for enzyme-catalyzed DNA C-to-U deamination in breast cancer (7). The DNA deaminase APOBEC3B was found to be upregulated and active in the

Authors' Affiliations: [1]Biochemistry, Molecular Biology and Biophysics Department; [2]Masonic Cancer Center, University of Minnesota, Minneapolis; [3]Division of Biomedical Statistics and Informatics, Department of Health Sciences Research; [4]Medical Genome Facility and Department of Laboratory Medicine and Pathology; [5]Department of Laboratory Medicine and Pathology; [6]Division of Medical Oncology, Department of Oncology; [7]Division of Epidemiology, Department of Health Sciences Research; [8]Division of Oncology Research, Department of Oncology; [9]Department of Molecular Pharmacology and Experimental Therapeutics, Mayo Clinic; [10]Women's Cancer Program, Mayo Clinic Cancer Center, Rochester, Minnesota; [11]Department of Cancer Biology, University of Kansas, Kansas City, Kansas; [12]Department of Obstetrics & Gynecology, University of Washington School of Medicine, Seattle, Washington; and [13]Illumina Cambridge Ltd, Chesterford Research Park, Little Chesterford, Cambridge, United Kingdom

Note: Supplementary data for this article are available at Cancer Research Online (http://cancerres.aacrjournals.org/).

B. Leonard and S.N. Hart contributed equally to this work.
H. Sicotte, S.H. Kaufmann, and R.S. Harris are co-senior authors of this work.

Corresponding Author: Reuben S. Harris, University of Minnesota, Department of Biochemistry, Molecular Biology and Biophysics, Minneapolis, MN 55455. Phone: 612-624-0457; Fax: 612-625-2163; E-mail: rsh@umn.edu

doi: 10.1158/0008-5472.CAN-13-1753

majority of breast cancer cell lines, and its upregulation in tumors correlated with increased C-to-T transition and overall base substitution mutation loads (7). APOBEC3B is one of seven APOBEC3 deaminases, which have broad and overlapping functions in providing innate immunity to a large number of DNA-based parasites, including retroviruses (with susceptible cDNA intermediates), some DNA viruses, and even naked foreign DNA (ref. 8, and references therein). These APOBEC3 enzymes are related to the antibody-diversification enzyme–activation-induced DNA cytidine deaminase (AID) and the *APOB* mRNA-editing protein APOBEC1 (9). All nine of these enzymes exhibit DNA deaminase activity in multiple assays. Furthermore, transgenic expression of AID and APOBEC1 can induce tumor formation in mice (10–12). In humans, AID is associated with B-cell tumorigenesis, imatinib resistance, and *BCL2* gain-of-function (13–16). However, because human AID and APOBEC1 are expressed predominantly in B lymphocytes and gastrointestinal tissues, respectively, it is unlikely that they contribute to tumorigenesis elsewhere. Based on the fact that breast and ovarian cancers have similar mutation spectra (17) and often show high degrees of genomic instability (2, 18), here we test the possibility that APOBEC3B is an active source of genomic DNA damage and mutagenesis in ovarian cancer.

Materials and Methods

Cell lines

A2780, IGROV-1, OVCAR3, OVCAR5, OVCAR8, OV17, OV167, OV177, OV202, PEO1, PEO4, and SKOV3IP were obtained from the Mayo Clinic ovarian cell line repository. SKOV3, ES2, and TOV-21G were provided by Dr. Martina Bazarro (University of Minnesota, Twin Cities, MN; details of all cell lines in Supplementary Table S1). RNA from IMCC3, 1816–686, 1816–575, IOSE-VAN, MA148, CAOV3, OVCA429, HEY, and OVCA433 were provided by Dr. Amy Skubitz (University of Minnesota, Twin Cities, MN). Normal fallopian tube epithelial lines were derived by culture of epithelial cells recovered from fimbria (resected at the University of Washington for non-neoplastic indications in accordance with the institutional-review-board–approved protocol 08#27077).

APOBEC expression profiling of cell lines

As specific antibodies for APOBEC3B are not yet available, quantitative reverse transcription-PCR (qRT-PCR) was used for mRNA quantification as described previously (7, 19, 20). RNA was isolated using the RNeasy Mini Kit (Qiagen, cat#74106). cDNA was prepared using the Transcriptor Reverse Transcriptase Kit (Roche, cat#03531287001), and qPCR was performed using 2× Probes Master Mix (Roche, cat # 04887301001). All primer and probe combinations are listed in Supplementary Table S2.

APOBEC3B knockdown experiments

Knockdowns were done using pLKO.1-based lentiviral vectors and techniques reported previously (7). Transduced cells were selected with 1 μg/mL puromycin for 1 week before being harvested for fractionation. APOBEC3B knockdown was confirmed by qRT-PCR, as above.

Clinical specimens

Review of hematoxylin and eosin (H&E)-stained slides by a gynecologic pathologist prior to both banking and analysis was performed on all samples (details of clinical specimens in Supplementary Tables S3–5). This ensured that the normal samples were tumor free and the tumor samples contained greater than 70% carcinoma cells. Whole-genome and RNA sequencing was applied to previously banked low-stage, high-grade ovarian carcinomas (Mayo Clinic, IRB#08-008535). qRT-PCR for *APOBEC* mRNA levels was performed, as described earlier, using previously banked ovarian carcinomas (Mayo Clinic, IRB#12-000095). All patients had provided prior written consent for the banking and subsequent research on their specimens, including genomic studies (Mayo Clinic, IRB#08-005749).

APOBEC expression profiling of ovarian tissues

Cryostat sections were cut into TRIzol (Invitrogen, cat#15596-026). Adjacent sections from the same block were examined by a pathologist after H&E staining to confirm greater than 70% tumor cell content. Normal ovaries (Supplementary Table S3), confirmed to be cancer-free by gross and microscopic examination at the time of harvest by a pathologist, were cryopreserved and sectioned in a similar fashion. Following TRIzol-based RNA extraction, cDNA synthesis and qRT-PCR were performed as described earlier.

Genomic sequencing and resequencing

After review of H&E-stained slides by a gynecologic pathologist, tumor and germline DNA was extracted using the Gentra Puregene Tissue Kit (Qiagen, cat # 158622) and sequenced on the Illumina GAIIX with 40× average coverage. Detailed methods used for mutation calling can be found in the Supplementary Materials. In addition, we performed resequencing of *TP53* by Sanger sequencing (21) and targeted capture sequencing in a subset of tumors and normal samples (3) to confirm *TP53* mutation status and validate a somatic *BRCA2* mutation in one tumor that had been identified in whole-genome sequences.

Statistical analyses

Statistically significant differences between normal and tumor tissue, high and low grade, and early and late stage were determined using the Wilcoxon rank sum test. The Wilcoxon signed rank test was used to analyze matched normal and tumor tissues. Association between *APOBEC3B* expression levels and mutation counts were examined graphically, with significance determined using Spearman correlation coefficients and *P*-values. Best-fit lines for mutation correlations were estimated using linear regression (Graphpad Prism v.5.0).

Results

APOBEC3B expression and localization in ovarian cancer cell lines

As an initial test for APOBEC3B in ovarian cancer, we used qRT-PCR to survey the mRNA levels of *APOBEC3B* and all of the

related deaminase family members in a panel of ovarian cancer cell lines (Fig. 1A; Supplementary Fig. S1 and Table S1). The expression level of each deaminase family member was normalized to that of the constitutive housekeeping gene *TATA binding protein* (*TBP*). This analysis revealed that *APOBEC3B* expression varied widely across these cell lines (Fig. 1A). In contrast, immortalized ovarian epithelial lines (OSE) used as controls showed a much narrower range of *APOBEC3B* expression (Fig. 1A). Ten of 18 [56%; 95% confidence interval (CI): 30.8–78.5%] ovarian cancer cell lines had *APOBEC3B* mRNA levels more than 3 SDs above the mean of the five OSE lines. Cultured fallopian tube epithelial cells (22), another normal control, had *APOBEC3B* levels similar to those found in the OSE lines (Fig. 1A).

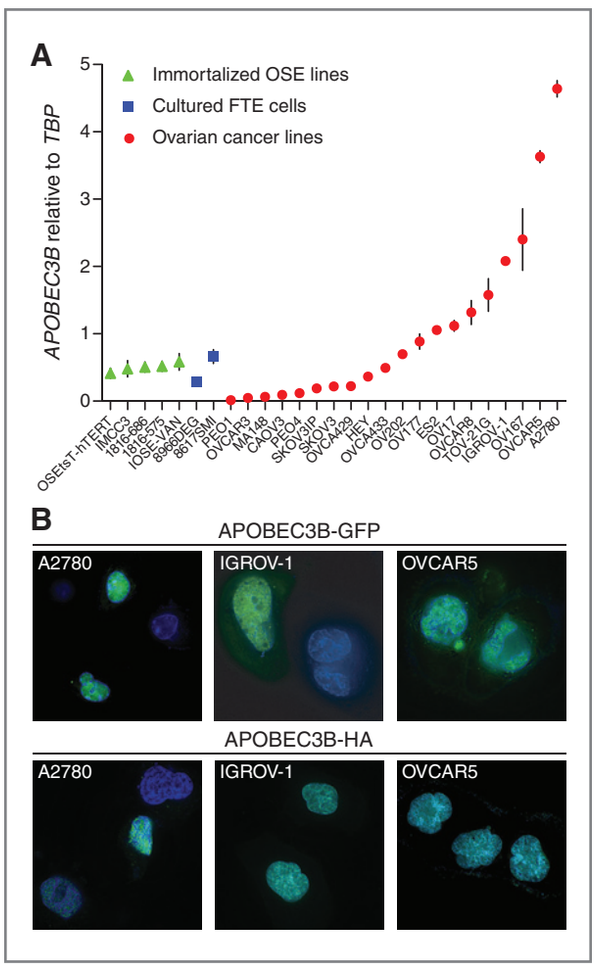

Figure 1. *APOBEC3B* expression and localization in ovarian cancer cell lines. A, *APOBEC3B* mRNA levels in the indicated ovarian cancer cell lines (red circles, $n = 18$ with sister pairs PEO1/4 and SKOV3/IP counted only once), fallopian tube epithelial (FTE) cells (blue squares, $n = 2$), and immortalized ovarian surface epithelium (OSE) cell lines (green triangles, $n = 5$). Each data point is the mean *APOBEC3B* level of three independent qRT-PCR reactions presented relative to mRNA levels of the constitutive housekeeping gene *TBP* (error bars, 1 SD). B, GFP and hemagglutinin (HA)-tagged APOBEC3B (green) colocalize with Hoechst-stained nuclear DNA (blue) in the indicated ovarian cancer cell lines. All images were taken at 60× magnification.

Examination of additional deaminase members revealed that mRNA of the most closely related family member, *APOBEC3A*, was undetectable in 16 out of 18 (88.9%, 95% CI 65.3–98.6%) ovarian cancer cell lines, consistent with its developmental confinement to myeloid lineage cell types (Supplementary Fig. S1; refs. 19, 20). Although some of the other family members were expressed to varying degrees in several of the ovarian cancer cell lines, none were overexpressed in the majority of lines based on the same statistical criteria (3 SDs over the mean level in the five OSE lines; Supplementary Fig. S1).

We next investigated whether APOBEC3B protein localizes to the nuclear compartment in ovarian cancer cell lines, as it does in several other cancer and immortalized cell lines (7, 23–28). Because specific antibodies for APOBEC3B are not yet available, we determined the localization of transfected APOBEC3B-eGFP in live ovarian cancer cells and APOBEC3B-HA in fixed and permeablized cell lines by fluorescence microscopy. Both APOBEC3B-eGFP and APOBEC3B-HA were predominantly nuclear in the OVCAR5, IGROV-1, and A2780 ovarian cancer cell lines (Fig. 1B). Taken together, these qRT-PCR and localization data suggested that APOBEC3B is positioned to pose a threat to ovarian genomic integrity.

Endogenous APOBEC3B activity in ovarian cancer cell lines

The gold standard for quantifying an endogenous protein is measuring its functional activity. We, therefore, assayed the endogenous DNA C-to-U deaminase activity in three of the highest and lowest *APOBEC3B*-expressing cell lines using a fluorescence-based assay (Fig. 2A and Supplementary Fig. S2). Clear endogenous DNA deaminase activity was detected from the *APOBEC3B*-high but not the -low expressing lines, suggesting a direct link. To ask which cellular compartment contained the source of this activity, we generated cytoplasmic and nuclear protein extracts from the *APOBEC3B*-high lines and assayed the activity of each fraction. High levels of single-stranded DNA C-to-U activity were detected in the nuclear, but not the cytoplasmic, protein fractions, consistent with localization data (Fig. 2B and C). To test whether this nuclear deaminase activity was specifically due to endogenous APOBEC3B, we also performed the experiments using protein extracts prepared from pools of cells transduced with control or *APOBEC3B* short hairpin RNAs (shRNA). Two independent knockdown constructs were used, with one causing stronger depletion of endogenous *APOBEC3B* mRNA levels (Fig. 2B, blue vs. green bars; ref. 7). The level of *APOBEC3B* knockdown correlated directly with loss of nuclear ssDNA C-to-U deaminase activity, with the stronger shRNA causing a larger diminution of activity (Fig. 2C). OVCAR5, IGROV-1, and A2780 yielded similar results.

In parallel, we also assessed the dinucleotide deamination preference of endogenous APOBEC3B in nuclear and cytoplasmic protein extracts from the same cell lines. In all instances, a single-stranded DNA substrate with a 5′-TC deamination target was strongly preferred over other dinucleotide-containing substrates (Fig. 2C and Supplementary Fig. S3). Taken together, these coupled genetic knockdown and

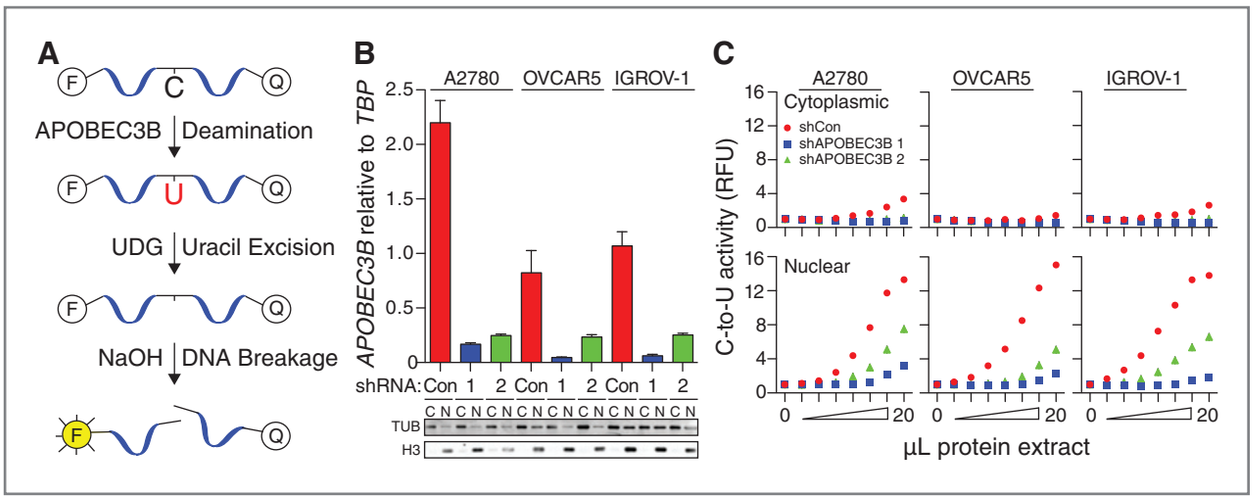

Figure 2. Endogenous APOBEC3B activity in ovarian cancer cell lines. A, a schematic of the fluorescence-based DNA cytosine deamination assay. The single-stranded DNA substrate has a target cytosine, 5′ fluorescent group (F) and 3′ fluorescence-quenching group (Q). Deamination and uracil excision create an abasic site, hydroxide breaks the DNA backbone, and the fluorescent group escapes quenching. B, *APOBEC3B* qRT-PCR data from the indicated ovarian cancer cell lines expressing control shRNA (Con) or one of two shRNAs specific to *APOBEC3B* (1 or 2; $n = 3$; mean and SD shown for each condition). Fractionation is confirmed by immunoblots of the cytoplasmic (C) and nuclear (N) protein fractions from each condition (TUB, anti-tubulin; H3, anti-histone H3). C, DNA C-to-U deaminase activity elicited by cytoplasmic (top) and nuclear (bottom) protein extracts from the indicated cell lines. These experiments used a single-stranded DNA substrate with a single 5′-TC deamination target. Symbol colors match the knockdown bar colors in B.

enzymatic activity experiments demonstrate that most, if not all, of the measurable DNA deaminase activity in the nuclear compartment of the tested ovarian cancer cell lines is due to the endogenous APOBEC3B enzyme.

Deamination kinetics of recombinant APOBEC3B

Deoxynucleotide identities immediately 5′ and 3′ of target DNA cytosines can strongly influence the efficiency of DNA deamination by APOBEC3 family members (7, 29–31). Therefore, to compare the cell-based studies (discussed earlier) with mutational data from clinical samples (discussed later), we determined the local sequence specificity and enzyme kinetics of recombinant APOBEC3B *in vitro*. Using the catalytic domain of APOBEC3B (residues 195–382) purified from HEK293 cells, we conducted a series of time-course experiments with substrates spanning all 16 permutations of deoxynucleotides immediately 5′ and 3′ of the target cytosine (i.e., 5′-NCN). Quantification of deamination products accumulating over time enabled catalytic efficiencies to be determined. These analyses revealed that the nucleotide directly 5′ of the target cytosine was a stronger determinant of APOBEC3B deamination than the 3′ nucleotide. More specifically, we found that 5′-TC dinucleotides support the highest reaction rates, and 5′-AC and 5′-GC support the lowest (representative gels in Fig. 3A and quantification in Fig. 3B). Overall, these *in vitro* preferences of recombinant APOBEC3B catalytic domain confirmed and extended our previous studies (7, 32), and they correlated strongly with and further validated results obtained with the full-length endogenous enzyme in nuclear extracts of breast (7) and ovarian cancer cell lines (this study, discussed in earlier sections). Importantly, these substrate preferences, which represent the intrinsic deamination activity of APOBEC3B, provided a hierarchy of "signatures" for comparison with the mutation patterns in ovarian cancer genomic mutation datasets described further.

APOBEC3B expression in ovarian tumors

To extend our studies to clinical ovarian cancer specimens, we initially assayed DNA deaminase family member mRNA expression in eight normal or benign ovarian tissues (Supplementary Table S3) and a series of 23 ovarian cancers, including 16 early-stage high-grade serous ovarian cancers that were also subjected to whole-genome sequencing (clinical characteristics in Supplementary Tables S4 and S5). High-quality RNA was prepared from flash-frozen tissues, and each of the deaminase family members were quantified by qRT-PCR as described earlier. As expected based on our cell line expression analysis, *APOBEC3B* mRNA varied widely in ovarian cancers, but was significantly upregulated in comparison with normal ovarian tissue as a control (tumor $n = 23$ vs. normal tissue $n = 8$; $P = 0.011$ by the Wilcoxon rank sum test; Supplementary Fig. S4). In addition, *APOBEC1* was upregulated in one tumor ($P = 0.006$), but this was considered a rare exception because it was not supported by cell line or additional tumor data. No significant differential expression was apparent for *APOBEC3A* ($P = 0.541$), *APOBEC3G* ($P = 0.068$), *APOBEC3H* ($P = 0.214$), *AID* ($P = 0.214$), or *APOBEC4* (0.107). Interestingly, lower levels were found in the tumor than in normal ovaries for *APOBEC3C* ($P = 0.002$), *APOBEC3D* ($P = 0.002$), *APOBEC3F* ($P = 0.040$), and *APOBEC2* ($P = 0.003$), suggesting either that these family members are downregulated in ovarian cancers or they are poorly expressed in cells that eventually develop into tumors (Supplementary Fig. S4).

Using the same qRT-PCR assay and the data from our initial cohort, we next examined *APOBEC3B* expression in an expanded panel of 77 ovarian tumors (clinical characteristics in

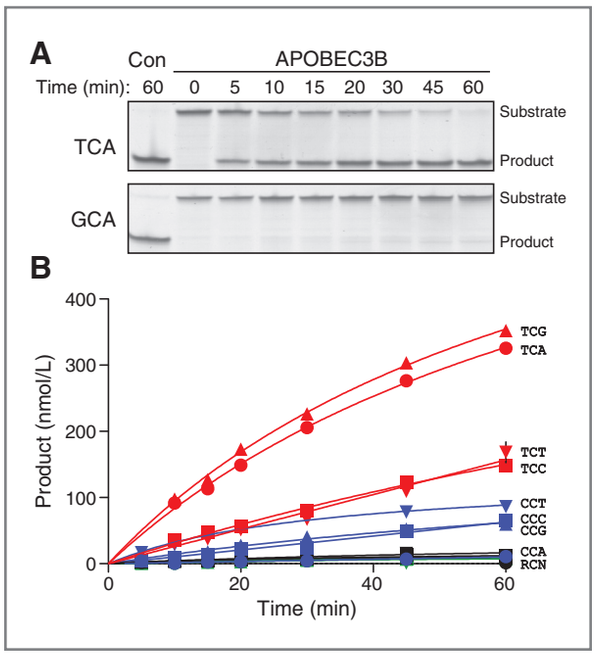

Figure 3. Intrinsic DNA deamination preferences of recombinant APOBEC3B. A, representative gel images of APOBEC3B catalytic domain DNA deamination products accumulating over the indicated reaction times for the 5′-TCA (most preferred) and 5′-GCA (least preferred) trinucleotide contexts. Complete deamination by APOBEC3A is shown as a positive control (Con). B, APOBEC3B catalytic domain deamination kinetics using 5′-TCN, CCN, GCN, and ACN single-stranded DNA substrates ($n = 16$ reaction conditions done each in triplicate; mean values are shown with SD smaller than symbols in all but one instance). Reactions with 5′-RCN substrates had indistinguishably low activity (R = A or G).

Supplementary Tables S4 and S5), and determined whether higher *APOBEC3B* correlates with stage and/or grade (Fig. 4A–D). *APOBEC3B* mRNA levels in most normal ovarian tissues were only a small fraction of those of the housekeeping gene *TBP* with an average of 0.07 ± 0.04 APOBEC3B/TBP ($n = 20$, excluding OV412 as an outlier; Dixon Q test confidence limit, 99%). Using a strict cutoff of 3 SD above the normal ovary tissue mean, we found that 44 of the 66 ovarian carcinomas without matched normal samples show upregulated *APOBEC3B* mRNA levels (66.7%; 95% CI, 55.3–78.1%; Fig. 4A). In addition, APOBEC3B was upregulated in nine of 11 instances where both matched normal and tumor tissue was available ($P = 0.010$ by Signed rank test; Fig. 4B). When comparing all 77 tumors, there was no statistical difference in *APOBEC3B* mRNA levels in late versus early-stage samples ($P = 0.222$ by Wilcoxon rank sum test; Fig. 4C), suggesting that APOBEC3B upregulation may occur early in ovarian cancer development. In contrast, there was a significant difference between grade 3 and all lower grade samples ($P = 0.044$ by the Wilcoxon rank sum test; Fig. 4D), suggesting that APOBEC3B may contribute to tumor dedifferentiation.

As in many cell-of-origin versus tumor comparisons, ovarian or fallopian tube epithelia comprise a small fraction of the tissue, while tumors are mostly epithelial. This factor is further affected by microenvironment changes that occur during tumor development. These and other factors complicate direct comparisons between normal tissues and tumor samples. Therefore, to fortify these comparisons, we performed an additional analysis using the mean *APOBEC3B* expression values from immortalized OSE lines (Fig. 1A) and expression values from the tumors described here (Fig. 4A). Similar to the analysis described earlier, *APOBEC3B* expression levels were at least 3 SD above the mean of the immortalized OSE cells in 12 of the 77 ovarian tumors. Therefore, regardless of the normal samples used for comparison, a subset of ovarian tumors show upregulated *APOBEC3B* expression levels.

Next, The Cancer Genome Atlas (TCGA) Network microarray and RNA sequencing (RNAseq) data were used to test the robustness of our qRT-PCR approach and to extend expression results to larger, independent datasets (Fig. 4E and F). TCGA microarray data were available for 581 ovarian cancers and eight unrelated normal ovarian tissues, and an analysis of these data indicated *APOBEC3A* and *APOBEC3B* upregulation in malignant tissues ($P < 0.0003$ by Mann–Whitney U test; Fig. 4E and Supplementary Table S6). However, the microarray result for *APOBEC3A* is likely a false-positive because five out of 11 *APOBEC3A* probes have more than 22/25 nucleotides of identity with *APOBEC3B*, and eight out of 11 *APOBEC3B* probes have more than 22/25 nucleotides of identity with *APOBEC3A* (7). Moreover, modest *APOBEC3G* downregulation is also a false positive because the probe set in question has no complementarity to *APOBEC3G*, and the second *APOBEC3G* probe set showed no significant difference. RNAseq data largely overcome these technical limitations because the longer paired-end reads enhance the chance of spanning a region of heterology and enabling the correct gene-specific assignment of sequence reads (7, 32). Analysis of the RNAseq data available on 188 TCGA samples demonstrated that the expression of *APOBEC3A* is lower than *APOBEC3B* in high-grade, late-stage serous ovarian cancer specimens, confirming that the *APOBEC3A* measurement on the microarray is likely a false positive (Supplementary Fig. S5). Moreover, quantification of *APOBEC3B* expression by RNAseq across the entire 188 TCGA ovarian cancer samples examined by this technique also yielded data that largely mirrored our qRT-PCR results (Fig. 4F). In addition, a subset of the samples analyzed by qRT-PCR was part of the TCGA studies ($n = 42$; denoted by asterisks in Fig. 4A and indicated in Supplementary Table S5). Analysis of the 32 TCGA samples analyzed by both qRT-PCR and RNAseq revealed a strong correlation between results obtained with both techniques ($P < 0.0001$, $r = 0.88$ by the Spearman correlation; Fig. 4G). This concordance lends confidence to the overall datasets, and fortifies the conclusion that *APOBEC3B* expression varies widely but appears to be elevated in many of the ovarian cancers studied relative to normal ovarian tissues or immortalized OSE samples used as controls in this study.

Mutation patterns in early-stage ovarian tumors

To gain further insight into the biologic consequences of varied APOBEC3B expression in ovarian cancer, we analyzed whole-genome sequences from 16 early-stage, mostly high-grade serous ovarian cancers (Supplementary Table S4) and

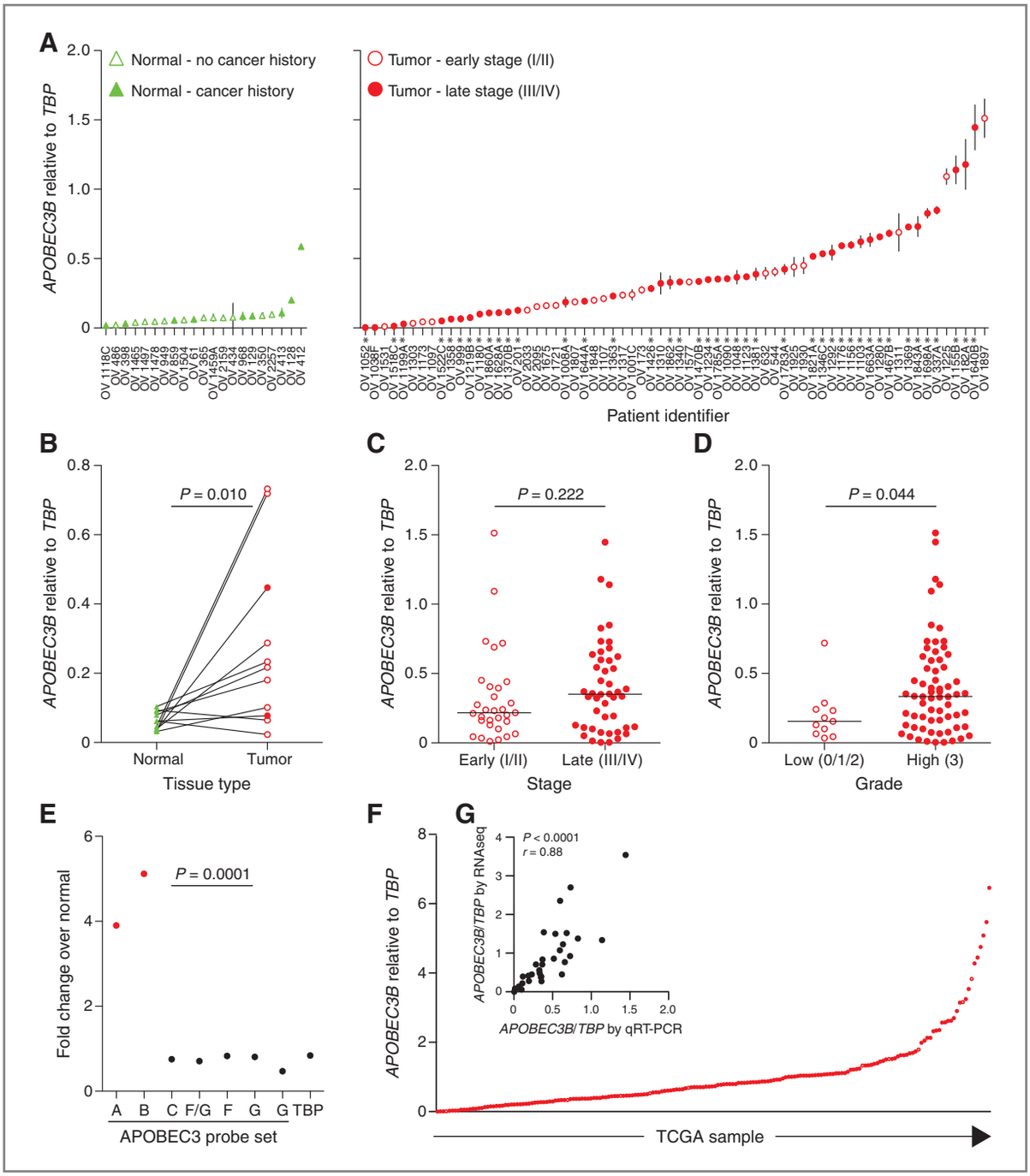

Figure 4. *APOBEC3B* expression in ovarian tumors. A, *APOBEC3B* levels in the indicated normal (green triangles; $n = 21$) and unmatched cancerous (red circles; $n = 66$) ovarian tissues. Cancer history is indicated by open (no history) or filled green symbols (some history; see Supplementary Tables S2 and S4 for additional patient information). Tumor stage is indicated by open (early-stage) or closed (late-stage) red symbols. Data points in each category are arranged from lowest to highest *APOBEC3B* expression level. Each point reports the mean *APOBEC3B* level of 3 independent qRT-PCR reactions presented relative to mRNA levels of the constitutive housekeeping gene *TBP* (error bars = 1 SD). Asterisks indicate samples that are also in TCGA data sets with the alternative identifiers listed in Supplementary Table S5. B, dot plot showing *APOBEC3B* expression in matched normal and tumor specimens ($n = 11$ unrelated to specimens in A). Lines connect matched specimens. *P* values were calculated using the Signed rank test. C and D, dot plots showing the relationship between *APOBEC3B* levels (as in A) and tumor stage (early vs. late) or tumor grade (low vs. high). *P* values were calculated using the Wilcoxon rank sum test. E, relative microarray *APOBEC3* expression levels based on data from the indicated probe sets. A false-positive *APOBEC3A* signal is expected due to high nucleotide identity with *APOBEC3B* and cross-hybridizing probe sets (see supplement to ref. 7). F, *APOBEC3B* quantification by RNA sequencing of 188 TCGA ovarian tumors. *APOBEC3B* mRNA levels are presented relative to those of the housekeeping gene *TBP* and plotted from lowest to highest. No normal tissues were available for comparison. G, a two-dimensional plot comparing qRT-PCR and RNA sequencing data for tumor samples common to each analysis ($n = 32$). *P* values calculated using the Spearman correlation.

examined the relationship between *APOBEC3B* expression and the mutations found in these cancers. Importantly, all patients were treatment naïve and had no evidence of other cancers prior to diagnosis. The total load of somatic mutations varied widely among the 16 early-stage serous ovarian cancers, with a range from 1,055 to 8,249 mutations per specimen (Supplementary Table S4). A significant positive correlation ($P = 0.013$, $r = 0.60$ by the Spearman correlation) was observed between mutation load and *APOBEC3B* levels (Fig. 5A). Approximately 60% of base substitutions occurred at C/G base pairs, which is notable given the A/T richness of the human genome.

Surprisingly, we found that the majority of mutations occurring at C/G base pairs in ovarian cancer are C-to-A or C-to-G transversions (Fig. 5B). Moreover, these transversions correlated with *APOBEC3B* expression levels (Fig. 5C). This finding was unexpected because the anticipated simplest outcome of a C-to-U genomic DNA lesion is a C-to-T transition through DNA replication or misrepair, as observed for breast cancer (see Discussion). Nevertheless, this transversion pattern is most likely due to the APOBEC3B enzymatic activity, as these events most frequently occurred within APOBEC3B-preferred 5′-TC motifs (Fig. 5D). The rarity of transversion mutation events at 5′-TCG sites may be due to a natural scarcity of CpG dinucleotides in the human genome (in comparison to other dinucleotides) and/or to the lower activity of APOBEC3B on 5-methyl-cytosine substrates in comparison with nonmethylated cytosines (by analogy to the closely related enzyme APOBEC3A; refs. 33, 34). Similar results were evident in the subset of genomic mutations confirmed by RNA sequencing (Fig. 5E–H). These mutation data are consistent with a model in which APOBEC3B catalyzed C-to-U genomic DNA deamination events are converted by uracil DNA glycosylase into abasic

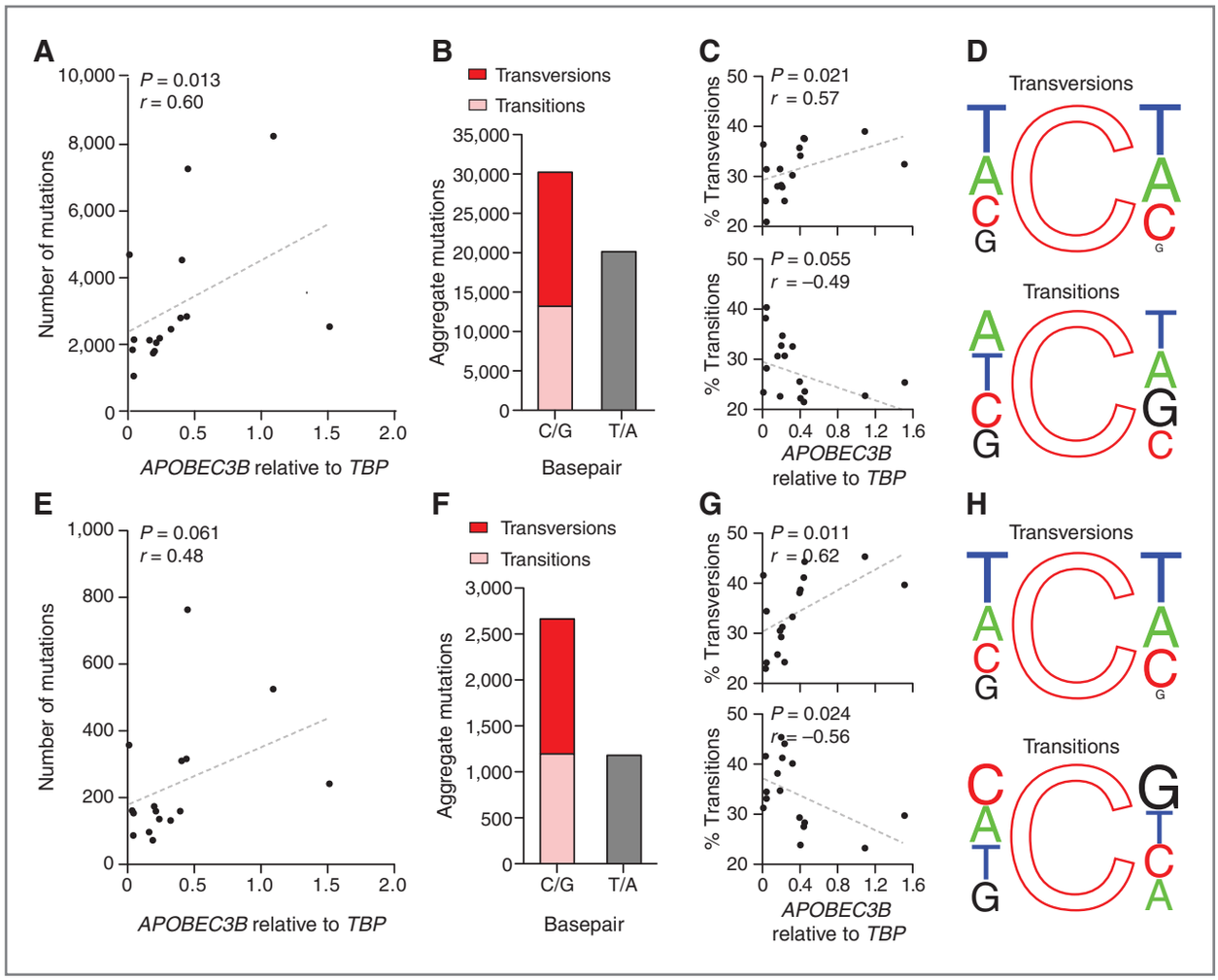

Figure 5. Ovarian cancer genomic mutation patterns. A, correlation between *APOBEC3B* expression and total mutation loads in whole-genome sequences of 16 early-stage serous ovarian carcinomas (Supplementary Table S4) assessed using the Spearman correlation. B, grouped analysis of whole-genome mutation types in all 16 cancers. C, correlation between *APOBEC3B* expression levels and mutation type at C/G base pairs in whole-genome sequences assessed using the Spearman correlation. D, trinucleotide context of the mutated C for transversions (top) and transitions (bottom) in whole-genome sequences (16,986 transversions and 13,232 transitions). E–H, as above for A–D, except these analyses were done using RNAseq-confirmed mutations from the same 16 early-stage serous ovarian carcinomas (1,468 transversions and 1,198 transitions).

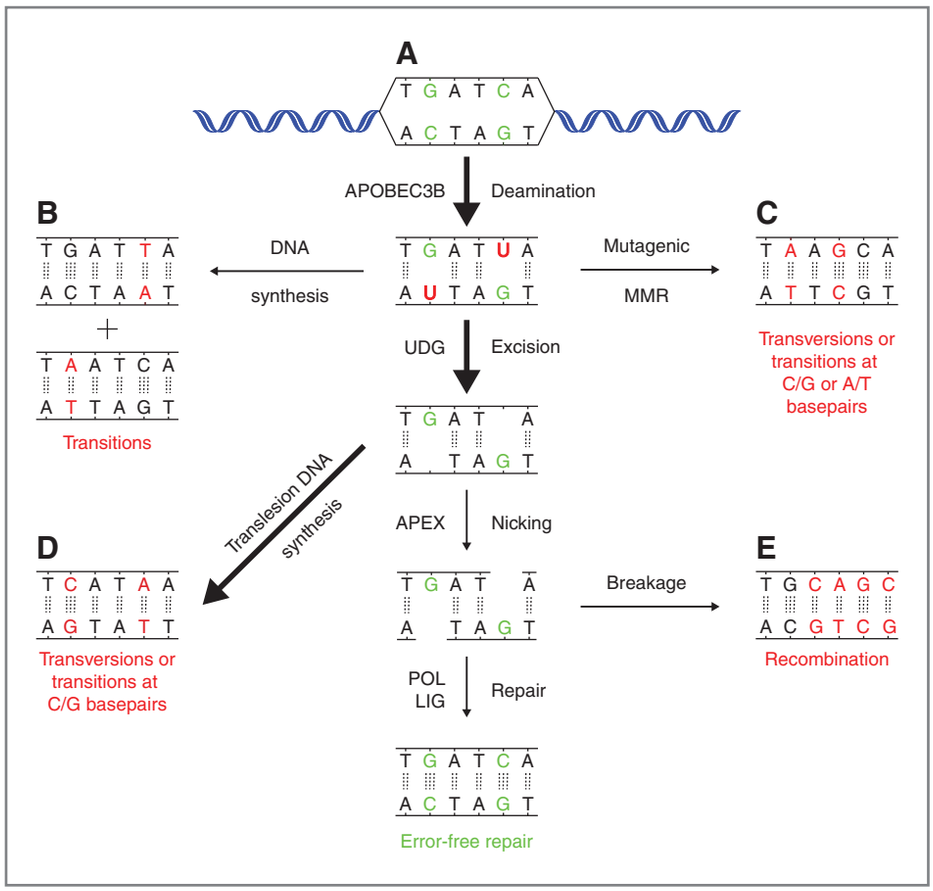

Figure 6. DNA deamination model for mutation in cancer. APOBEC3B catalyzed C-to-U deamination events in single-stranded DNA can be repaired error-free (A) or processed in an error-prone manner by DNA synthesis (B, D), mutagenic repair (C), or recombination (E). This model is based in part on our prior studies (7) and on the DNA deamination mechanism for antibody gene diversification (14, 38).

sites, which template the misinsertion of T or C through error-prone DNA synthesis, and ultimately yield C-to-A or C-to-G transversions (after at least one round of DNA replication or repair; model in Fig. 6 discussed further).

Discussion

In this study, we have shown that *APOBEC3B* expression levels vary widely in ovarian cancer cell lines and clinical samples and are, in a substantial proportion of samples, higher than those in OSE lines, fallopian tube epithelial (FTE) cultures, or normal ovarian tissues. Knockdown experiments established that APOBEC3B was the only detectable source of DNA cytosine deaminase activity in nuclear extracts from multiple ovarian cancer cell lines. Microscopic images showed that epitope-tagged APOBEC3B is predominantly nuclear, in full agreement with the subcellular fractionation and activity studies of endogenous APOBEC3B. Biochemical experiments revealed the intrinsic cytosine deamination preferences for the catalytic domain of APOBEC3B and, interestingly, the preferred motif, 5′-TC, corresponds to the most abundant sites of C-to-A or C-to-G transversion mutations observed in whole-genome sequencing of early-stage serous ovarian cancer genomic DNA. Importantly, *APOBEC3B* expression levels correlated with mutational load in these tumors, suggesting a potential role for this enzyme in generating mutagenic lesions in ovarian cancer.

A unique finding here is the significant correlation between *APOBEC3B* expression levels, *in vitro* APOBEC3B deamination preferences, and the cytosine transversion signatures in early-stage ovarian cancers. In breast cancer, we recently reported a correlation between endogenous *APOBEC3B* expression and transition mutations at C/G base pairs, which can be easily explained by replication past uracil lesions (Fig. 6B; ref. 7). Concordant results were observed when APOBEC3B was overexpressed exogenously in HEK293 cells (7, 35). In contrast, the C-to-A and C-to-G transversions that predominate here are more complicated outcomes of an initiating genomic C-to-U lesion. The presence of these mutational events in ovarian cancer strongly suggests a model in which genomic uracils are converted by uracil DNA glycosylase into abasic sites, which in turn become substrates for error-prone translesion DNA synthesis (TLS; Fig. 6D). Several translesion DNA polymerases are strong candidates for such a role in generating transversion mutations downstream of cytosine deamination, including REV1, which elicits a strong preference for pyrimidine insertion opposite an abasic lesion (36). Indeed, such a model is supported by recent studies in yeast, which showed that both UNG and REV1 proteins are required for heterologous expression of human AID/APOBEC3 proteins to cause transversion mutations (37). Somatic hypermutation of immunoglobulin gene variable regions initiated by AID-dependent C-to-U deamination events also provides precedent that

enzyme-catalyzed uracil lesions can result in all six types of base substitutions (14, 38). In particular, in mouse models, the AID-induced C-to-A and C-to-G events are largely dependent upon the uracil excision enzyme UNG2 and most likely involve translesion synthesis polymerases (14, 38).

The transversions observed here in early-stage ovarian cancers in an APOBEC3B-preferred dinucleotide context raises many additional questions for future studies, including identifying the causal TLS polymerase (because humans have many more than yeast), explaining the differential processing of APOBEC3B-dependent lesions in different tumor types (e.g., breast vs. ovary), and addressing whether other mutagenic outcomes may also be APOBEC3B-dependent. For instance, incomplete repair of even a single uracil lesion can lead to a nicked DNA strand and, together with DNA replication (or even local synthesis), result in double-strand breaks that, in turn, are known to precipitate larger scale chromosomal aberrations such as insertions, deletions, duplications, and translocations (Fig. 6E). Thus, the elevated APOBEC3B expression documented here might also contribute to some of the larger-scale genomic alterations that are characteristic of many advanced serous ovarian tumors (2). Another critical point to address in future studies is assessing the effect of APOBEC3B expression on clinical outcomes, such as overall and progression-free survival, response to therapy, and rate of recurrence. To do this, large cohorts of clinical specimens with well-documented patient histories will need to be examined.

Recently, three separate analyses of large data collections examined the relationship between mutation pattern, mutation load, and *APOBEC* expression across multiple tumor types, including ovarian cancer (32, 39, 40). Although these analyses showed evidence for APOBEC-driven mutagenesis in multiple tumor types, none focused on ovarian cancer. This may be due to the fact that ovarian cancer has more modest *APOBEC3B* expression levels and mutation loads in comparison with some of these other cancers. The present study is the first to focus on ovarian cancer and differs from these recent reports in many ways: (i) we used specific qRT-PCR assays to profile *APOBEC3B* in ovarian cancer cell lines and tissues; (ii) we performed experiments to show that APOBEC3B is active in the nuclear compartment of ovarian cancer cell lines; (iii) we studied the relationship between *APOBEC3B* expression and mutation burden among individual ovarian cancers rather than across tumor types; and (iv) we examined mutation burden using newly available early-stage ovarian cancer whole-genome sequences. The results shown here suggest that these earlier studies may have been limited by both the specificity of the techniques used to measure gene expression and the limitations of exomic as opposed to whole-genome sequencing. Moreover, our work emphasizes the importance of in-depth studies of specific tumor types that may be overlooked by global analyses.

Disclosure of Potential Conflicts of Interest

No potential conflicts of interest were disclosed.

Authors' Contributions

Conception and design: B. Leonard, J.B. Nikas, D. Bently, R.K. Cheetham, S. Humphray, L.C. Hartmann, H. Sicotte, S.H. Kaufmann, R.S. Harris

Development of methodology: B. Leonard, S.N. Hart, A. Rathore, J.B. Nikas, R.K. Cheetham, J-B. Fan, H. Sicotte, R.S. Harris

Acquisition of data (provided animals, acquired and managed patients, provided facilities, etc.): B. Leonard, M.A. Carpenter, J.B. Nikas, E.K. Law, W.L. Brown, D.A. Bell, C. April, M. Bibikova, J-B. Fan, R. Grocock, S. Humphray, Z. Kingsbury, J. Chien, E.M. Swisher, L.C. Hartmann, K.R. Kalli, E.L. Goode, S.H. Kaufmann

Analysis and interpretation of data (e.g., statistical analysis, biostatistics, computational analysis): B. Leonard, S.N. Hart, M.B. Burns, N.A. Temiz, R.I. Vogel, J.B. Nikas, Y. Li, Y. Zhang, M.J. Maurer, A.L. Oberg, D.A. Bell, R.K. Cheetham, R. Grocock, S. Humphray, J. Peden, E.M. Swisher, E.L. Goode, H. Sicotte, R.S. Harris

Writing, review, and/or revision of the manuscript: B. Leonard, S.N. Hart, R. I. Vogel, J.B. Nikas, A.L. Oberg, J.M. Cunningham, V. Shridhar, J. Chien, E.M. Swisher, K.R. Kalli, H. Sicotte, S.H. Kaufmann, R.S. Harris

Administrative, technical, or material support (i.e., reporting or organizing data, constructing databases): B. Leonard, A. Rathore, J.B. Nikas, W.L. Brown, R.K. Cheetham, J. Peden, L.C. Hartmann

Study supervision: B. Leonard, L.C. Hartmann, S.H. Kaufmann, R.S. Harris

Other (All research of microarray databases and bioinformatic analysis of all microarray data): J.B. Nikas

Acknowledgments

The authors thank M. Bazarro for cell lines, A. Skubitz for cell line RNA, P. Schneider for isolating tumor RNA, and several laboratory members for helpful discussions.

Grant Support

The work in the Harris laboratory was financially supported in part by seed grants from the Minnesota Ovarian Cancer Alliance and the University of Minnesota Clinical and Translational Science Institute (supported by NIH grant no. 1UL1RR033183). R.I. Vogel, N.A. Temiz, and J.B. Nikas were supported by NIH P30 CA77598 utilizing the Biostatistics and Bioinformatics Core shared resource of the Masonic Cancer Center, University of Minnesota. M.B. Burns was supported by a Department of Defense Breast Cancer Research Program Predoctoral Fellowship (BC101124). M.A. Carpenter was supported by NIH F32 GM095219. The work of the Mayo Clinic Ovarian Cancer Research Program was supported by NIH P50 CA136393, NIH P30 CA15083, R01 CA122443, an Ovarian Cancer Research Fund Program Project Development Grant, and a grant from the Fred C. and Katherine B. Andersen Foundation.

The costs of publication of this article were defrayed in part by the payment of page charges. This article must therefore be hereby marked *advertisement* in accordance with 18 U.S.C. Section 1734 solely to indicate this fact.

Received June 25, 2013; revised September 4, 2013; accepted September 21, 2013; published OnlineFirst October 23, 2013.

References

1. Siegel R, Naishadham D, Jemal A. Cancer statistics, 2012. CA Cancer J Clin 2012;62:10–29.
2. TCGA. Integrated genomic analyses of ovarian carcinoma. Nature 2011;474:609–15.
3. Walsh T, Casadei S, Lee MK, Pennil CC, Nord AS, Thornton AM, et al. Mutations in 12 genes for inherited ovarian, fallopian tube, and peritoneal carcinoma identified by massively parallel sequencing. Proc Natl Acad Sci U S A 2011;108:18032–7.
4. Kelland L. The resurgence of platinum-based cancer chemotherapy. Nat Rev 2007;7:573–84.
5. Markman M. Antineoplastic agents in the management of ovarian cancer: current status and emerging therapeutic strategies. Trends Pharmacol Sci 2008;29:515–9.
6. Norquist B, Wurz KA, Pennil CC, Garcia R, Gross J, Sakai W, et al. Secondary somatic mutations restoring BRCA1/2 predict chemotherapy resistance in hereditary ovarian carcinomas. J Clin Oncol 2011;29:3008–15.
7. Burns MB, Lackey L, Carpenter MA, Rathore A, Land AM, Leonard B, et al. APOBEC3B is an enzymatic source of mutation in breast cancer. Nature 2013;494:366–70.

8. Harris RS, Hultquist JF, Evans DT. The restriction factors of human immunodeficiency virus. J Biol Chem 2012;287:40875–83.
9. Conticello SG. The AID/APOBEC family of nucleic acid mutators. Genome Biol 2008;9:229.
10. Pasqualucci L, Bhagat G, Jankovic M, Compagno M, Smith P, Muramatsu M, et al. AID is required for germinal center-derived lymphomagenesis. Nat Genet 2008;40:108–12.
11. Yamanaka S, Balestra ME, Ferrell LD, Fan J, Arnold KS, Taylor S, et al. Apolipoprotein B mRNA-editing protein induces hepatocellular carcinoma and dysplasia in transgenic animals. Proc Natl Acad Sci U S A 1995;92:8483–7.
12. Okazaki IM, Hiai H, Kakazu N, Yamada S, Muramatsu M, Kinoshita K, et al. Constitutive expression of AID leads to tumorigenesis. J Exp Med 2003;197:1173–81.
13. Klemm L, Duy C, Iacobucci I, Kuchen S, von Levetzow G, Feldhahn N, et al. The B cell mutator AID promotes B lymphoid blast crisis and drug resistance in chronic myeloid leukemia. Cancer Cell 2009;16:232–45.
14. Robbiani DF, Nussenzweig MC. Chromosome translocation, B cell lymphoma, and activation-induced cytidine deaminase. Annu Rev Pathol 2013;8:79–103.
15. Lohr JG, Stojanov P, Lawrence MS, Auclair D, Chapuy B, Sougnez C, et al. Discovery and prioritization of somatic mutations in diffuse large B-cell lymphoma (DLBCL) by whole-exome sequencing. Proc Natl Acad Sci U S A 2012;109:3879–84.
16. Schuetz JM, Johnson NA, Morin RD, Scott DW, Tan K, Ben-Nierah S, et al. BCL2 mutations in diffuse large B-cell lymphoma. Leukemia 2012;26:1383–90.
17. Greenman C, Stephens P, Smith R, Dalgliesh GL, Hunter C, Bignell G, et al. Patterns of somatic mutation in human cancer genomes. Nature 2007;446:153–8.
18. TCGA. Comprehensive molecular portraits of human breast tumours. Nature 2012;490:61–70.
19. Refsland EW, Stenglein MD, Shindo K, Albin JS, Brown WL, Harris RS. Quantitative profiling of the full *APOBEC3* mRNA repertoire in lymphocytes and tissues: implications for HIV-1 restriction. Nucleic Acids Res 2010;38:4274–84.
20. Stenglein MD, Burns MB, Li M, Lengyel J, Harris RS. APOBEC3 proteins mediate the clearance of foreign DNA from human cells. Nat Struct Mol Biol 2010;17:222–9.
21. Hong GF. Sequencing of large double-stranded DNA using the dideoxy sequencing technique. Biosci Rep 1982;2:907–12.
22. Smith NL, Welcsh P, Press JZ, Agnew KJ, Garcia R, Swisher EM. E2F3b over-expression in ovarian carcinomas and in BRCA1 haploinsufficient fallopian tube epithelium. Genes Chromosomes Cancer 2012;51:1054–62.
23. Bogerd HP, Wiegand HL, Doehle BP, Lueders KK, Cullen BR. APOBEC3A and APOBEC3B are potent inhibitors of LTR-retrotransposon function in human cells. Nucleic Acids Res 2006;34:89–95.
24. Stenglein MD, Harris RS. APOBEC3B and APOBEC3F inhibit L1 retrotransposition by a DNA deamination-independent mechanism. J Biol Chem 2006;281:16837–41.
25. Stenglein MD, Matsuo H, Harris RS. Two regions within the amino-terminal half of APOBEC3G cooperate to determine cytoplasmic localization. J Virol 2008;82:9591–9.
26. Pak V, Heidecker G, Pathak VK, Derse D. The role of amino-terminal sequences in cellular localization and antiviral activity of APOBEC3B. J Virol 2011;85:8538–47.
27. Lackey L, Demorest ZL, Land AM, Hultquist JF, Brown WL, Harris RS. APOBEC3B and AID have similar nuclear import mechanisms. J Mol Biol 2012;419:301–14.
28. Lackey L, Law EK, Brown WL, Harris RS. Subcellular localization of the APOBEC3 proteins during mitosis and implications for genomic DNA deamination. Cell Cycle 2013;12:762–72.
29. Rausch JW, Chelico L, Goodman MF, Le Grice SF. Dissecting APOBEC3G substrate specificity by nucleoside analog interference. J Biol Chem 2009;284:7047–58.
30. Kohli RM, Maul RW, Guminski AF, McClure RL, Gajula KS, Saribasak H, et al. Local sequence targeting in the AID/APOBEC family differentially impacts retroviral restriction and antibody diversification. J Biol Chem 2010;285:40956–64.
31. Wang M, Rada C, Neuberger MS. Altering the spectrum of immunoglobulin V gene somatic hypermutation by modifying the active site of AID. J Exp Med 2010;207:141–53.
32. Burns MB, Temiz NA, Harris RS. Evidence for APOBEC3B mutagenesis in multiple human cancers. Nat Genet 2013;45:977–83.
33. Carpenter MA, Li M, Rathore A, Lackey L, Law EK, Land AM, et al. Methylcytosine and normal cytosine deamination by the foreign DNA restriction enzyme APOBEC3A. J Biol Chem 2012;287:34801–8.
34. Wijesinghe P, Bhagwat AS. Efficient deamination of 5-methylcytosines in DNA by human APOBEC3A, but not by AID or APOBEC3G. Nucleic Acids Res 2012;40:9206–17.
35. Shinohara M, Io K, Shindo K, Matsui M, Sakamoto T, Tada K, et al. APOBEC3B can impair genomic stability by inducing base substitutions in genomic DNA in human cells. Sci Rep 2012;2:806.
36. Kim N, Mudrak SV, Jinks-Robertson S. The dCMP transferase activity of yeast Rev1 is biologically relevant during the bypass of endogenously generated AP sites. DNA Repair (Amst) 2011;10:1262–71.
37. Taylor BJ, Nik-Zainal S, Wu YL, Stebbings LA, Raine K, Campbell PJ, et al. DNA deaminases induce break-associated mutation showers with implication of APOBEC3B and 3A in breast cancer kataegis. Elife 2013;2:e00534.
38. Di Noia JM, Neuberger MS. Molecular mechanisms of antibody somatic hypermutation. Annu Rev Biochem 2007;76:1–22.
39. Roberts SA, Lawrence MS, Klimczak LJ, Grimm SA, Fargo D, Stojanov P, et al. An APOBEC cytidine deaminase mutagenesis pattern is widespread in human cancers. Nat Genet 2013;45:970–6.
40. Alexandrov LB, Nik-Zainal S, Wedge DC, Aparicio SA, Behjati S, Biankin AV, et al. Signatures of mutational processes in human cancer. Nature 2013;500:415–21.